A Hybrid Prognostics Approach for MEMS: from Real Measurements to Remaining Useful Life Estimation

Haithem Skima, Kamal Medjaher, Christophe Varnier, Eugen Dedu, Julien Bourgeois

A Hybrid Prognostics Approach for MEMS: from Real Measurements to Remaining Useful Life Estimation

H. Skima[a,*], K. Medjaher[b,*], C. Varnier[a], E. Dedu[a], J. Bourgeois[a]

[a] *FEMTO-ST Institute, UMR CNRS 6174 - UFC / ENSMM, 25000 Besançon, France*
[b] *Production Engineering Laboratory (LGP), INP-ENIT, 65000 Tarbes, France*

Abstract

This paper presents a hybrid prognostics approach for Micro Electro Mechanical Systems (MEMS). This approach relies on two phases: an offline phase for the MEMS and its degradation modeling, and an online phase where the obtained degradation model is used with the available data for prognostics. In the online phase, the particle filter algorithm is used to perform online parameters estimation of the degradation model and predict the Remaining Useful life (RUL) of MEMS. The effectiveness of the proposed approach is validated on experimental data related to an electro-thermally actuated MEMS valve.

Keywords: Prognostics and health management, MEMS, degradation modeling, health assessment, fault prognostics, remaining useful life

1. Introduction

Nowadays, MEMS devices are used in several industrial segments such as automotive, medical and aerospace, where they contribute to achieve important tasks. However, reliability of MEMS is one of their major concerns [1]. They suffer from various failure mechanisms, which impact their performance, their availability and reduce their lifetime. Due to the significance of such aspect, several research works dealing with the reliability of MEMS have been published,

*Corresponding author
Email addresses: haithem.skima@femto-st.fr (H. Skima), kamal.medjaher@enit.fr (K. Medjaher)

such as [2, 3, 4, 5, 6]. The most used methodology to study the reliability of MEMS was proposed by the *Sandia National Laboratories* [7, 8]. The aim of this methodology is to improve the reliability of MEMS based on the identification and the comprehension of their failure mechanisms and the definition of their predictive reliability model.

Improving reliability of MEMS devices has several advantages, such as increasing their lifetime and improving their availability. Nevertheless, reliability still has some limitations. It is defined as *the ability of a product or system to perform as intended (i.e., without failure and within specified performance limits) for a specified time, in its life cycle conditions* [9]. According to this definition, reliability is valid only for given conditions and a period of time. This is the case, for example, for cars which are guaranteed by automobile manufacturers for a period of time in given operating conditions. In this situation, the reliability is estimated without taking into account the specific utilization of each car (driver profile, environment conditions, roads quality, frequency of use, etc.). However, in practice, the lifetime should be different from one car to another depending on how and where it is used. Furthermore, the predictive reliability models are obtained from statistical data on representative samples. These models, which are generic for all the samples, are not updated during the utilization. This means that, once they are estimated, the model parameters still constant while they should change due to the factors mentioned previously.

Prognostics and Health Management (PHM) can be a solution to address the above limitations. PHM is the combination of six layers that collectively enable linking failure mechanisms with life management (Fig. 1). It makes use of past, present, and future operating conditions in order to assess the health state of the system, diagnose its faults, update the degradation models parameters, anticipate failures by predicting the RUL and improve decision making to prolong the lifetime of the system. Within the framework of PHM, prognostics is considered as the core activity. It is defined by the PHM community as the estimation of the RUL of physical systems based on their current health state and their future operating conditions.

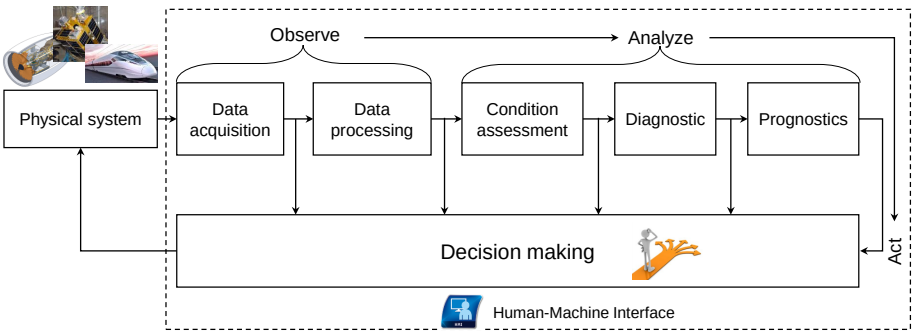

Figure 1: Prognostics and Health Management cycle.

Prognostics can be done according to three main approaches: 1) model-based (also called physics-of-failure), 2) data-driven and 3) hybrid (or fusion) prognostics approaches. The first approach deals with the prediction of the RUL of systems by using mathematical representation to formalize physical understanding of a degrading system, and includes both system modeling and physics-of-failures (PoF) [10]. The second approach aims at transforming raw monitoring data (temperature, vibration, current, voltage, etc.) into relevant information, which are used to learn models for health assessment and RUL prediction [10]. Finally, the third approach combines both previous approaches and benefits from both to overcome their drawbacks. Prognostics results obtained by this approach are claimed to be more reliable and accurate [11].

Although its benefits are well proven, there are few contributions addressing fault prognostics of MEMS [1, 12]. To fill this gap, a hybrid prognostics approach for MEMS is proposed in this paper. Furthermore, and in order to demonstrate its performance, the proposed approach is applied to an electro-thermally actuated MEMS valve. All the steps of the approach are performed: from measurements acquisition to RUL estimation.

The rest of the paper is structured as follows. Section 2 presents the proposed prognostics approach. The main steps of the implementation of the used prognostics tool are summarized in Section 3. The effectiveness of the proposed approach is demonstrated in Section 4, based in an application to a MEMS

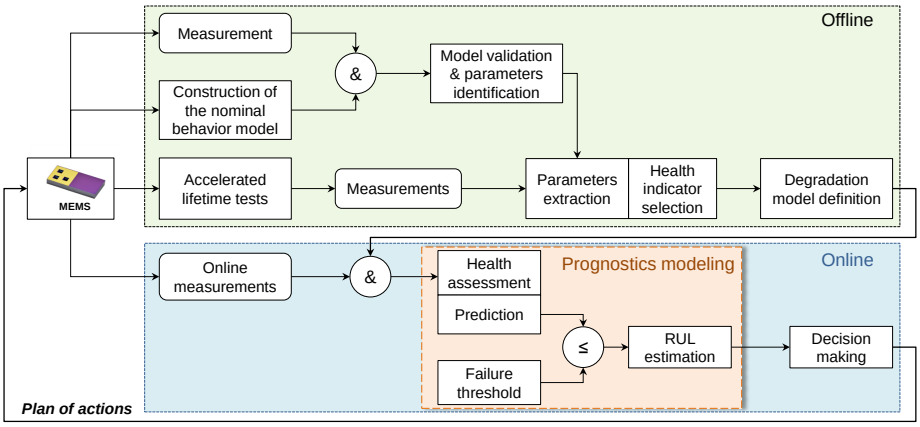

Figure 2: Overview of the proposed hybrid prognostics approach.

device. Finally, conclusions are drawn in Section 5.

2. Proposed hybrid prognostics approach

The proposed prognostics approach, presented in Fig. 2, can be applied on different categories of MEMS at a condition that the following assumptions hold.

1. The instrumentation needed to monitor the behavior of MEMS (sensors, camera, etc.) is available

2. Sufficient knowledge about the studied MEMS is available to derive their nominal behavior models and identify their failure mechanisms, which may take place during their utilization.

The prognostics approach relies on two phases: an offline phase to construct the nominal behavior model of the MEMS, select a physical health indicator (HI) and derive its degradation model, and an online phase where the obtained degradation model is used for future behavior prediction and RUL estimation. The principal steps of the approach are explained hereafter.

- *Nominal behavior model construction*: it can be obtained by writing the corresponding physical laws of the targeted MEMS or derived experimentally. Its complexity depends on the modeling assumptions made during its construction. The parameters of the model can be identified by exciting the MEMS and getting its time response. In other cases, these parameters can be obtained from the manufacturer's specifications. In this paper, the nominal behavior model is obtained by writing the corresponding physical laws, which are then validated experimentally.

- *Degradation model*: it can be obtained experimentally through accelerated lifetime tests or given by experts. In this work, the degradation model is related to drifts of the physical parameters of the MEMS (friction coefficient, stiffness, etc.). These drifts are considered as Health Indicators (HI) and are obtained by analyzing the data acquired from tests by using appropriate modeling tools (regression, curve fitting, etc.).

- *Accelerated lifetime test*: it is an aging of a product that induces normal failures / degradation in a short amount of time by applying stress levels much higher than normal ones (strain, temperature, voltage, vibration, pressure, etc.). The main interest is to observe the time evolution to predict the life span. According to Matmat *et al.* [13], the simplest and most useful accelerated lifetime test to derive the degradation model of a MEMS is to stress it by applying a square signal (cycling).

- *Prognostics modeling*: prognostics is divided into two main stages: learning and prediction. In the learning stage, the prognostics tool combines the available data with the degradation model to learn the behavior of the system and estimate the parameters of its degradation model. This stage lasts until a prediction is required at time t_p. Then, in the prediction stage, the prognostics tool propagates the state of the system and determines at what time the failure threshold (FT) is reached. In practice, the FT can be set either experimentally, by observing the time evolution of the HI, or given by an expert. In this paper, it is set according to a

desired performance that we defined. The performance criteria can correspond to the stability, the rapidity, the precision, etc. It can also be related to a decrease (or an increase) of the system's parameters such as its compliance. Note that, the FT does not necessarily indicate a complete failure of the system, but a faulty state beyond which there is a risk of functionality loss [14]. Finally, the RUL is calculated as the difference between the failing time t_f and the starting prediction time t_p (Eq. 1).

$$RUL = t_f - t_p \tag{1}$$

In the offline phase, the time evolution of the selected HI is approximated by a mathematical model to define the degradation model. In the online phase, the parameters of the degradation model are unknown and need to be estimated as a part of the prognostics process. To do so, the particle filter algorithm can be used. It allows propagating the state and managing uncertainties in the model parameters and the prognostics phase. Besides that, its allows handling non-linear and non-Gaussian situations.

3. Failure prognostics based on particle filtering

In the literature, several research works dealing with the particle filtering method and its application to the prognostics were published. For more theoretical details, interested readers can refer to the work published by Arulampalam *et al.* [15]. Consequently, this section aims at summarizing the main steps which allow to understand the implementation of the particle filter for failure prognostics of MEMS and to easily reproduce the proposed approach.

3.1. Particle filtering framework

The particle filter was introduced in 1993 as a numerical approximation to the nonlinear / non-Gaussian recursive Bayesian estimation problem [16]. The problem of recursive Bayesian estimation is defined by two equations: the first considers the evolution of the system state $\{x_k, k \in \mathbb{N}\}$ which is given by

$$x_k = f(x_{k-1}, \lambda_{k-1}) \tag{2}$$

where k is the time step index, f is the transition function from the state x_{k-1} to the next state x_k and $\{\lambda_{k-1}, k \in \mathbb{N}\}$ is the independent identically distributed process noise sequence. The objective is to recursively estimate x_k from measurements introduced by the measurement model $\{z_k, k \in \mathbb{N}\}$

$$z_k = h(x_k, \mu_k) \tag{3}$$

where k is the time step index, h is the measurement function and $\{\mu_k, k \in \mathbb{N}\}$ is the independent identically distributed measurement noise sequence.

The main aim of the recursive Bayesian estimation problem is to recursively estimate the state of the system by constructing the Probability Density Function (PDF) of the state at time k based on all available information, $p(x_k|z_{1:k})$.

It is assumed that the initial PDF of the state vector, also called the *prior*, is available ($p(x_0|z_0) = p(x_0)$). The PDF $p(x_k|z_{1:k})$, known as the *posterior*, can be obtained recursively in two main stages: prediction and update.

Suppose that the required PDF $p(x_{k-1}|z_{1:k-1})$ at time $k-1$ is available.

- *Prediction stage:* in this stage the state model (Eq. 2) is used to obtain the prior PDF of the state at time k via the Chapman-Kolmogorov equation:

$$p(x_k|z_{1:k-1}) = \int p(x_k|x_{k-1})p(x_{k-1}|z_{1:k-1})dx_{k-1} \tag{4}$$

- *Update stage:* when a new measurement z_k becomes available, one can update the prior PDF via the Bayes rule

$$p(x_k|z_{1:k}) = \frac{p(z_k|x_k)p(x_k|z_{1:k-1})}{p(z_k|z_{1:k-1})} \tag{5}$$

This gives the formal solution to the recursive Bayesian estimation problem. Analytic solutions to this problem are available in a restrictive set of cases, including the Kalman filter, which assumes that the state and measurement models are linear and λ_k and μ_k are additive Gaussian noise of known variance. When these assumptions are unreasonable, which is the case in many applications, and the equations (Eq. 4) and (Eq. 5) cannot be solved analytically,

approximations are necessary. One of the most used approximate solution for this kind of problem is the particle filtering.

The particle filtering solution is a sequential Monte-Carlo method which consists in representing the required posterior PDF by a set of samples, also called particles, with associated weights and computing estimates based on these samples and weights. Different versions of particle filtering are reported in the literature. In this paper, we focus on the Sampling Importance Re-sampling (SIR) particle filer, which is commonly used in the prognostics field [17, 18, 19]. To explain the steps of the SIR algorithm, let suppose that at time step $k = 0$, the initial distribution $p(x_0)$ is approximated in the form of a set of N_s samples $\{x_0^i\}_{i=1}^{N_s}$ with associated weights $\{w_0^i = \frac{1}{N_s}\}_{i=1}^{N_s}$. Then, the following three steps are repeated until the end of the process:

- *Prediction:* a new PDF is obtained by propagating the particles from state $k-1$ to state k using the state model.
- *Update:* when a new measurement is available, the likelihood of the particles $p(z_k|x_k^i)$ is computed. This probability shows the degree of matching between the prediction and the measurement. Its calculation allows updating the weight of each particle.
- *Re-sampling:* this step appears to avoid a degeneracy of the filter. The basis idea of re-sampling is to eliminate the particles with small weights and duplicate the particles with large weights. The re-sampling step involves generating a new set of particles $\{x_k^{i*}\}_{i=1}^{N_s}$ by re-sampling (with replacement) N_s time from an approximate discrete representation of $p(x_k|z_{1:k})$. Surveys of re-sampling methods for particle filtering can be found in [20]. In this work, the systematic re-sampling method is used since it is simple to implement and offers good results [21].

3.2. RUL estimation based on particle filtering

In prognostics, the particle filter is used for the learning and prediction stages. During the learning stage, the behavior of the system is learned and

the unknown parameters of the state model are adjusted consequently. When a prediction is required, at time t_p, the posterior PDF given by $\{x_p^i, w_p^i\}_{i=1}^{N_s}$ is propagated until x^i reaches the failure threshold at t_f^i. The RUL PDF is then given by calculating $t_f^i - t_p$. The different steps of the prognostics using the particle filter are summarized in Fig. 3

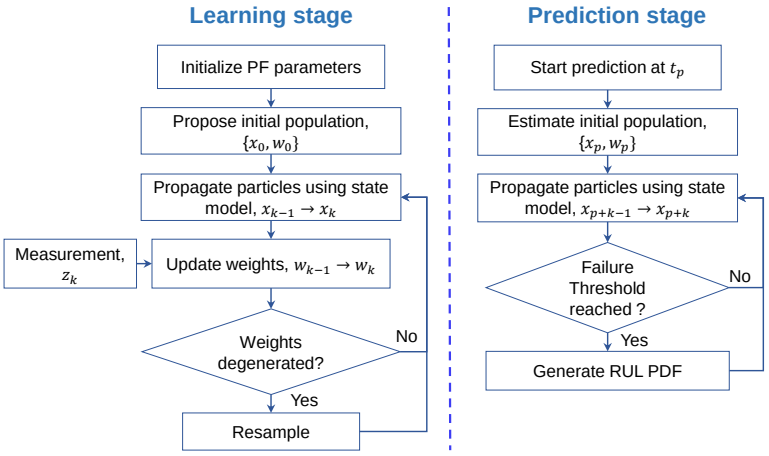

Figure 3: Particle filter framework for prognostics (adapted from [22]).

In the next section, an application of the proposed prognostics approach to a MEMS device is presented. The SIR particle filter algorithm is used to perform online prognostics.

4. Application and results

4.1. System description

The targeted device consists of an electro-thermally actuated MEMS valve of DunAn Microstaq, Inc. (DMQ), company (Fig. 4(a)). It is designed to control flow rates or pressure with high precision at ultra-fast time response ($<< 100\,ms$). It is currently being used in a number of applications in air conditioning and refrigeration, hydraulic control and air pressure control.

The valve is composed of three silicon layers. The center layer is a movable membrane. The other two layers of silicon act as interface plates to either elec-

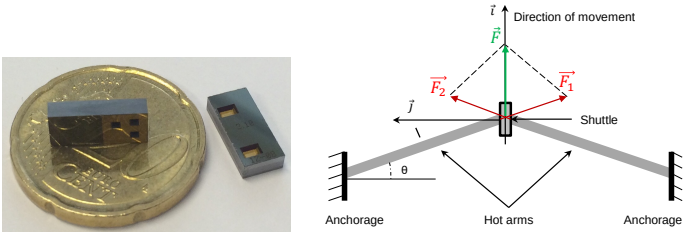

(a) (b)

Figure 4: (a) Electro-thermally acuated MEMS valve and (b) schematic view of its electro-thermal actuator.

trical connections (top layer) or fluid connection ports (bottom layer): common port, normally closed and normally open. The maximum actuation voltage of the valve is $12V$.

4.2. Nominal behavior model construction

The actuator used inside the targeted MEMS is an electro-thermal actuator. This actuator, presented in Fig. 4(b), is composed of hot arms inclined to the horizontal axis by an angle θ and clamped to the substrate and the freestanding central shuttle. When a voltage difference is applied across the anchor sites, heat is generated along the beams due to ohmic dissipation. The hot arms expand to push ahead symmetrically on the central part of the actuator (the shuttle). This part moves in the direction shown in Fig. 4(b). The shuttle is connected to the membrane and its movement allows moving the membrane to open or close the fluid ports.

$\overrightarrow{F_1}$ and $\overrightarrow{F2}$ are the two forces generated by the thermal displacement which act at the end of the hot arms. They are given by the following equation:

$$\|\overrightarrow{F_1}\| = \|\overrightarrow{F_2}\| = EAh\Delta T \tag{6}$$

where E is the Young's modulus, A is the surface of the arm section, h is the thermal expansion coefficient and ΔT is the temperature variation.

The resultant force $\overrightarrow{F}$ can be written as the sum of the two forces $\overrightarrow{F_1}$ and $\overrightarrow{F2}$ and the projection along $(\overrightarrow{i}, \overrightarrow{j})$ leads to the following equation:

$$\begin{cases} \overrightarrow{F_i} = F_1 \overrightarrow{i} + F_2 \overrightarrow{i} = 2EAh\Delta T sin(\theta) \overrightarrow{i} \\ \overrightarrow{F_j} = F_1 \overrightarrow{j} + F_2 \overrightarrow{j} = \overrightarrow{0} \end{cases} \tag{7}$$

The electro-thermal actuator is modeled as a mass-spring-damper (MSD) system. The application of the second fundamental law of dynamics leads to the following equation:

$$M\overrightarrow{a} = \sum \overrightarrow{F_{ext}} = \overrightarrow{F_f} + \overrightarrow{F_r} + \overrightarrow{F} \tag{8}$$

where $\overrightarrow{a}$ is the acceleration, $\overrightarrow{F_f} = -f\dot{x}\overrightarrow{i}$ is the friction force, $\overrightarrow{F_r} = -kx\overrightarrow{i}$ is the restoring force, $\overrightarrow{F} = 2EAh\Delta T sin(\theta)\overrightarrow{i}$ is the resultant displacement force, x is the displacement, f is the friction coefficient, k_s is the stiffness and M is the mass.

$$M\ddot{x} + f\dot{x} + k_s x = 2EAh\Delta T sin(\theta) \tag{9}$$

Due to the small size of the actuator, the inertial term $M\ddot{x}$ can be neglected in Eq. 9 with regard to the other forces [23]. The validity of this assumption will be discussed in Subsection 4.3. Based on this assumption, the dynamic model simplifies to:

$$f\dot{x} + k_s = 2EAh\Delta T sin(\theta) \tag{10}$$

To find a relation between the temperature variation ΔT and the input of the system (voltage U), we measured ΔT for different values of U (from $0\,V$ to $12\,V$). The temperature of the MEMS valve is measured by using a PT100 RTD sensor. A linear approximation of the evolution of ΔT as a function of U (Fig. 5) leads to the following expression:

$$\Delta T = \alpha U = 7.4U \tag{11}$$

By integrating this expression in the dynamic model, the following equation is obtained:

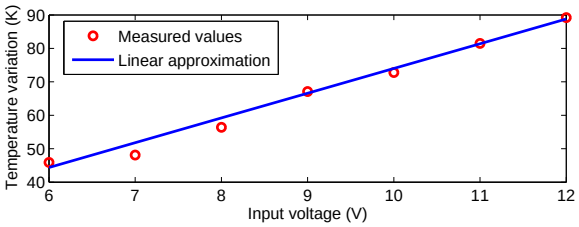

Figure 5: Temperature variation as a function of the input voltage.

Table 1: Numerical values used to calculate the constant β.

Parameter	**Symbol**	**Value**	**Unit**
Young's modulus	E	170	GPa
Section	A	200	μm^2
Angle of inclination	θ	10	$^\circ$
Thermal expansion coefficient	h	2.5×10^{-6}	K^{-1}

$$f\dot{x} + k_s = 2EAhsin(\theta)\alpha U = \beta U \tag{12}$$

where $\beta = 2EAhsin(\theta)\alpha$ is a constant. In β, two parameters are unknown, which are A and θ. The values of these two parameters are not given by the manufacturer and cannot be identified from the time response of the MEMS. Then, two values for these two parameters are assumed based on other works dealing with the design and manufacture of electrothermal actuators. The assumed values do not have an influence on the shape of the degradation curve. Table 1 shows the numerical values of all the parameters to calculate the constant β.

By applying the Laplace transform on Eq. 12, we derive the transfer function given in Eq. 13:

$$\frac{X(p)}{U(p)} = \frac{K}{1 + \tau p} \tag{13}$$

where $K = \dfrac{\beta}{k_s}$ is the static gain and $\tau = \dfrac{f}{k_s}$ is the time constant.

The obtained transfer function corresponds to a first order system. In the next subsection, this model is validated experimentally and its parameters are identified. These parameters are used in this approach to select a HI, which allows to track the degradation of the MEMS.

4.3. Experimental setup and tests

In order to validate the nominal behavior model and perform accelerated lifetime tests to generate the degradation model of the MEMS valve, we designed and built an experimental platform (Fig. 6). It is composed of five main parts:

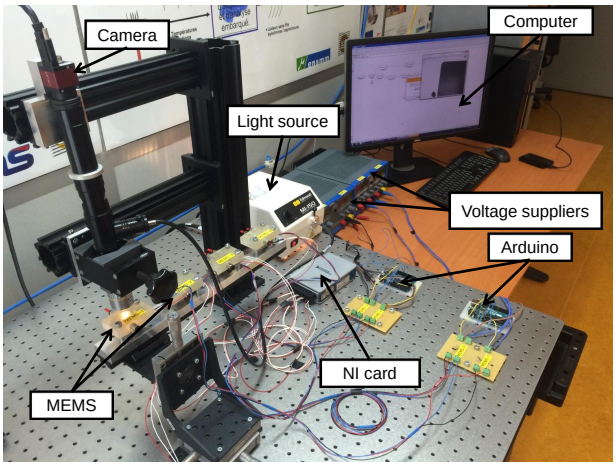

Figure 6: Overview of the experimental platform.

1. *The MEMS and its environment*: each MEMS is fixed on a support composed of a plastic part made by 3D printer, a metal plate to allow heat dissipation as the MEMS heats a lot, input-output of air connected to the fluid connection ports and an electronic card for power supply. The MEMS is attached on the metal plate under the electronic card by using silicone (Fig. 7).

2. *Power supply part*: it is composed of two voltage suppliers and two Arduino Uno cards. The cards are used as a switch to cycle the MEMS with

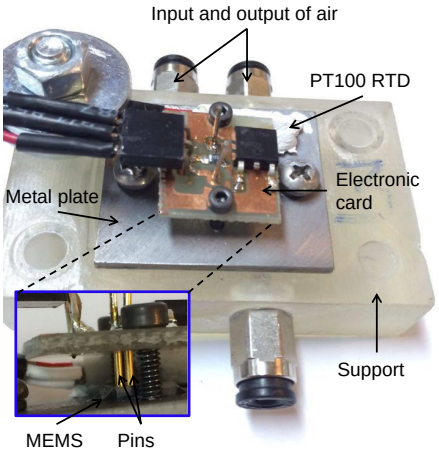

Figure 7: Support designed to fix the MEMS.

the desired frequency.

3. *Image acquisition part*: image acquisition is accomplished by a "Guppy Pro F-031" camera with a frame rate equal to 100 frames per second (fps) and a light source for the camera to allow seeing the movement of the membrane inside the MEMS. The communication between the computer and the camera is ensured by a FireWire B cable. The ensemble of images taken by the camera with a Matlab image-processing algorithm (Algorithm 1) allow measuring the displacement of the membrane of the MEMS and getting its time response.

4. *Temperature acquisition part*: the temperature of the MEMS is measured by using a PT100 RTD sensor attached on the metal plate. The communication between the PT100 RTD and the PC is ensured by a National Instrument card (NI 9216) and a Labview interface.

5. *Pneumatic part*: this part is composed of an air supply, an air filter and a pressure regulator.

To better show the different parts, a global synoptic of the experimental platform is given in Fig. 8. To minimize the mechanical vibration, the experimental

Algorithm 1 Pseudo-code of the Matlab image-processing algorithm.

```
1: function Displacement ()
2: Init: PxToMicroM ← CameraCalibration(); {conversion from pixel to μm}
3: Init: X ← 0; {displacement}
4: Init: Y ← 0;
5: Init: j ← 0;
6: Init: displacement[] ← 0;
7: while (1) do
8:    I ← GrabImage();
9:    FindContour(I);
10:   FindContourCentroid(I);
11:   (X,Y) ← CentroidPosition(I);
12:   X ← X * PxToMicroM;
13:   displacement[j] ← X;
14:   j ← j + 1;
15: end while
16: Plot(displacement);
17: end function
```

platform is placed on an anti-vibration table.

Before performing accelerated lifetime tests, one has to set the voltage value, which will be applied to the MEMS. For this purpose, static tests were conducted by increasing gradually the voltage (from $1\,V$ to $12\,V$) to find the displacement for various applied voltage values. Based on that, the voltage chosen is this application to perform accelerated lifetime tests is equal to $8\,V$. This value is not too high to not bring up prematurely degradation and not too low to obtain enough displacement.

Fig. 9 shows an example of an obtained time response of one MEMS valve supplied by a periodic square signal of $8\,V$ magnitude and $1\,Hz$ frequency. This time response is typical of a first order system and this confirms that the inertia can be neglected. The identification of the system parameters is based on the

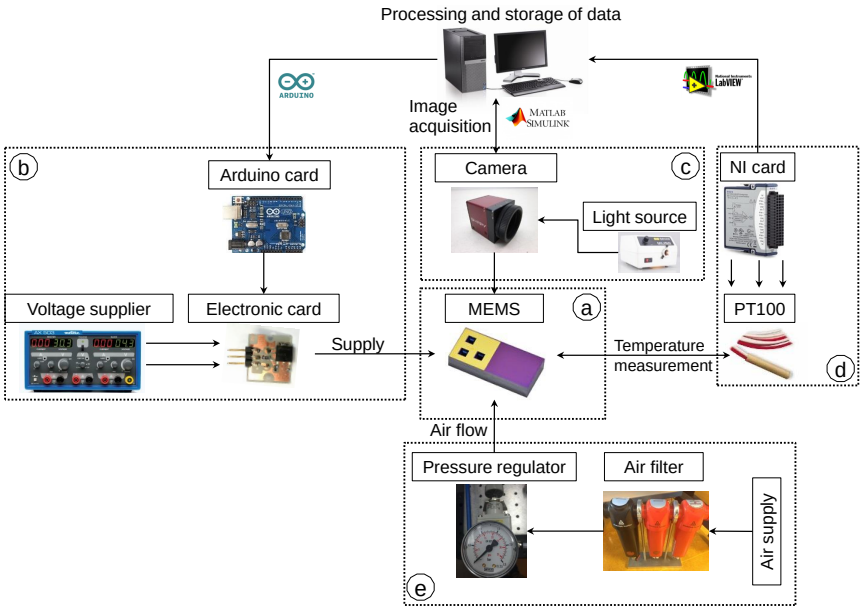

Figure 8: Global synoptic of the experimental platform.

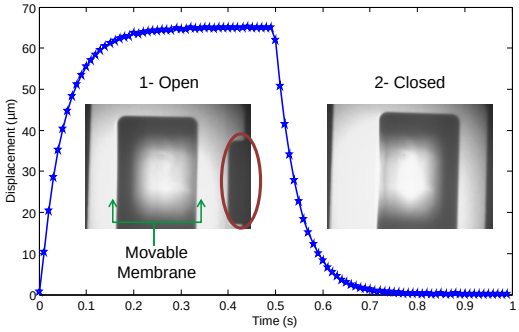

Figure 9: Time response of the MEMS valve. The two images of the membrane, 1 and 2, are taken by the camera through the normally closed port. At $8\,V$, the membrane moves (image 1) to create an output or an input of the air (circled part). At $0\,V$, the membrane returns to its initial position (image 2).

same experimental measurements and the modeling described in Section 4.2. By using Matlab *system identification toolbox*, the transfer function can be obtained and all the system parameters can be easily identified. The time evolution of all the identified parameters will be used to select a HI. The transfer function

corresponding to the time response presented in Fig. 9 is given in Eq. 14 and the identified parameters are given in Table 2.

$$\frac{X(p)}{U(p)} = \frac{8.02}{1 + 0.052p} \tag{14}$$

Table 2: Numerical values of the identified parameters of the system (these values concern only an example of measurement).

Parameter	**Symbol**	**Value**	**Unit**
Displacement	D	65	μm
Current	I	0.5	A
Static gain	K	8.02	$\mu m/V$
Time constant	τ	0.052	s
Stiffness	k_s	2.7×10^{-2}	N/m
Compliance	C	37.03	m/N
Friction coefficient	f	1.4×10^{-3}	Ns/m

Accelerated lifetime tests consist in cycling continuously four MEMS valves (Fig. 6). They are supplied by a periodic square signal of $8\,V$ magnitude and $1\,Hz$ frequency. The measurements acquisition is the same for all the tested MEMS. For each one of them the following steps are applied: 1) adjust the MEMS below the camera using a 3D positioner until having a very clear image, 2) get the time response by using the Matlab image-processing algorithm, 3) identify the parameters of the system by using the Matlab *system identification toolbox*, which leads to the transfer function of the obtained time response, and 4) store the results in different files in a dedicated computer for later use. Note that, the operating conditions and load were kept constant during the cycling tests.

4.4. Degradation model

To get the degradation model of the MEMS, the accelerated lifetime tests remained running for approximately three months, where the MEMS valves were continuously cycled. During this period, measurements were collected regularly. The raw results of the performed tests are presented in Fig. 10. The decrease in the magnitude of the displacement is related to the degradation in the tested MEMS valves. Among the identified parameters, the compliance C (inverse of the stiffness) has the same time evolution as the displacement (Fig. 11). Therefore, the compliance is selected as the physical HI, which can be used to track the degradation of the MEMS valves. The projection of this HI can be exploited to predict the future behavior of each MEMS valve and calculate its RUL.

To reduce variability of the raw experimental data and to remove different peaks, smoothing process is performed to capture important trends. This step is met by applying a robust local regression filter *rloess* (or robust locally weighted scatter plot smooth method) with a span value equal to 0.4 (i.e., 40 % of the total number of data points in the data set). Basically, *rloess* is a popular smoothing method based on robust locally weighted regression function and a second degree polynomial. Given scattered data, *rloess* filter can compute the robust weight for each data point in the span, which is resistant to outliers (it allocates lower weights to outliers). Fig. 12 shows the filtered experimental data using *rloess* filter.

By using the curve fitting method, the time evolution of the HI is approximated by a double exponential model, which represents the degradation model of the MEMS valves:

$$HI(t) = aexp(bt) + cexp(dt) \tag{15}$$

The numerical values of the exponential models parameters (a, b, c and d) for the four tested MEMS valves are given in Table 3. The coefficient of determination (R^2) values obtained from the curve fitting demonstrate that the double exponential model fits well the data.

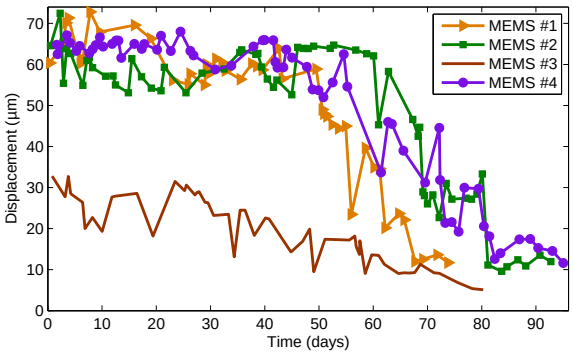

Figure 10: Experimental results: displacement as a function of time.

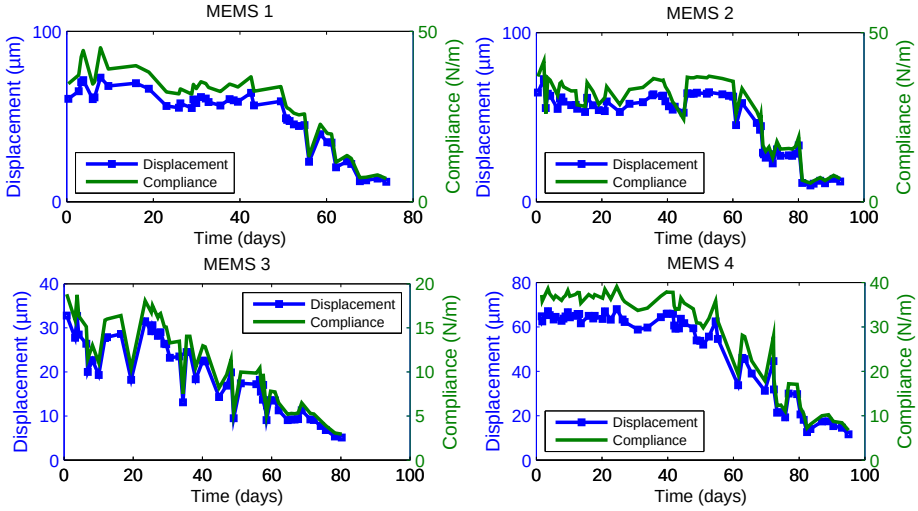

Figure 11: Displacement and compliance as a function of time.

The four tested MEMS valves have the same form of the degradation model (Eq. 15), but with different values of the parameters. Thus, this model is set as a generic degradation model for the studied MEMS valve.

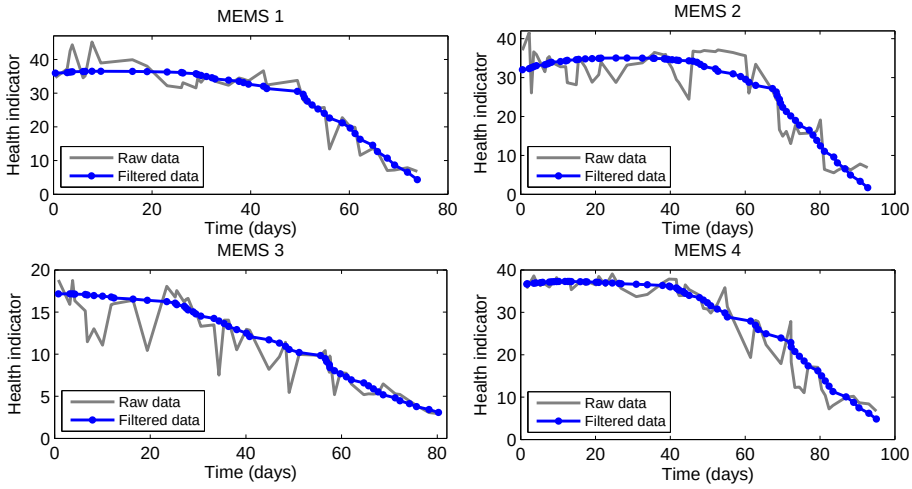

Figure 12: Filtering raw experimental data using *rloess*.

4.5. Prognostics modeling and results

To integrate the degradation model in the particle filter, the first step is to write it in a recursive form to create the state model:

$$HI(t_k) - HI(t_{k-1}) = aexp(bt_k) + cexp(dt_k) - aexp(bt_{k-1})) - cexp(dt_{k-1})$$
$$HI(t_k) = HI(t_{k-1}) + aexp(bt_k)(1 - exp(-b)) + cexp(d.t_k)(1 - exp(-d)) \quad (16)$$

We note that no additive noise is added to the model as in the theoretical form. We consider that the uncertainty of measures is included in the parameters

Table 3: Numerical values of the exponential models parameters .

Parameter	**MEMS #1**	**MEMS #2**	**MEMS #3**	**MEMS #4**
a	$-1.025.10^4$	$-8.47.10^4$	$-3.727.10^5$	$4.041.10^6$
b	0.0168	0.0157	0.0073	0.0116
c	$1.029.10^4$	$8.48.10^4$	$3.727.10^5$	$-4.041.10^6$
d	0.0167	0.0157	0.0073	0.0116
R^2	0.993	0.989	0.989	0.992

of the model identified by the filter. Regarding the measurement model, the experimental data are used in the filter. We assume that the additive noise is unknown and its variance is managed by the filter as described in [18].

4.5.1. Filter settings

The first step of the filter settings is the creation of the initial distributions for the state and the model parameters (a, b, c and d). The initial distribution of the state is centered on the first measured compliance value ($HI(t = 0)$). The noise induced by the measurement instruments and the form of the distribution are not known. In this case, we chose an uniform distribution centered on the initial measured value with a dispersion of $\pm 0.05 HI(t = 0)$. For the unknown parameters, an uniform distribution is also defined for each of them. The value on which each distribution is centered is obtained by fitting the model to the data.

Finally, the number of particles to be used must be defined. The larger it is, the better should be the prediction. However, a significant number of particles leads to a long calculation time. By refining the initialization of the model parameters, it is possible to use fewer particles. Pitt *et al.* [24] proposed a methodology to choose that number of particles. This methodology consists in launching the filter several times to create statistics and choose the appropriate number of particles. We applied the same methodology to define this number. The results obtained below were obtained using 5000 particles. This number provides good predictions with a reasonable calculation time.

4.5.2. Prognostics results

The RUL estimation of each MEMS requires a definition of a corresponding FT. In this case study, the FT is set as the point at which the HI value decreases by 60 %. Obviously, this value can change depending on the desired performance of the MEMS.

As explained in Section 3.2, prognostics is divided into two stages: learning and prediction. During the learning stage, the state of the MEMS (PDF of the

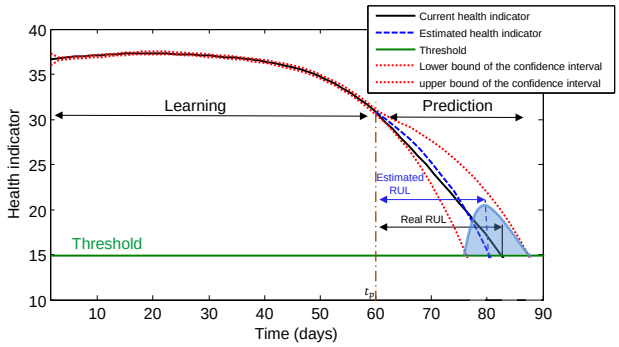

(a) RUL estimation at 60 days.

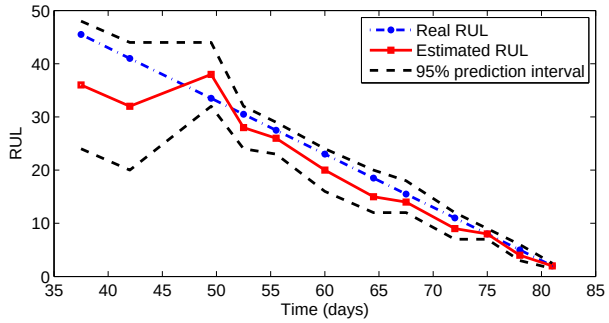

(b) RUL estimation at frequent intervals.

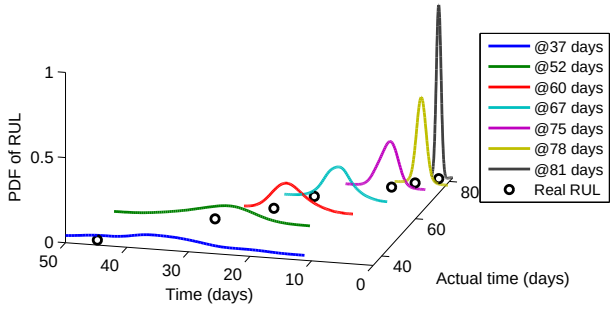

(c) Evolution of the RUL PDF

Figure 13: Prognostics results and RUL uncertainties.

HI) at time step k is estimated using the degradation model and the state at time step $k-1$. The parameters of the state model are consequently adjusted. Note that, the measurement model is not needed since measurements of the HI are available. These measurements are used in the update stage of the particle

filter to update the weights of the particles. This process lasts until a prediction is required at t_p. At this time, the estimated PDF of the HI is propagated until it reaches the FT at t_f. The duration between t_f and the starting point of prediction t_p gives the PDF of the RUL.

The settings described above is used to perform predictions of the health state and RUL. To construct the time evolution of the RUL, the prediction is launched at several time intervals (12 lengths of learning data). Fig. 13(a) gives a prediction made with a length of learning data of 60 days. The estimated health indicator is represented with a confidence interval to compare with the actual values. The estimated RUL corresponds to the median of the RUL PDF. The median RUL is chosen rather than the mean RUL since it gives early estimates and has better accuracy when more data are available. Note that, in PHM context, it is better to have early estimates rather than late RUL to avoid late maintenance interventions [25]. The particle filter allows managing uncertainty of long-term predictions and the confidence to facilitate decision making either offline for maintenance or online for control or system configuration.

Fig. 13(b) shows the estimated RUL at frequent intervals compared to the real one. One can clearly see that the accuracy of the RUL estimates increases with time, as more data are available. Furthermore, the real RUL values are within the prediction interval at the different time steps. Finally, the uncertainties in RUL estimation decreases as time passes. This is shown in Fig. 13(c), which represents the time evolution of the RUL PDF (only some PDFs are drawn to make a readable figure). For example, at time equal to 37 days, we have a flat distribution of RUL, whereas at time equal to 81 days we have a sharp one. This evolution of the RUL PDF explains the increase of the prediction accuracy in time. These obtained results demonstrate the accuracy and the significance of the proposed prognostics approach.

5. Conclusion

A hybrid prognostics approach is proposed in this paper. First, the architecture of this approach and its different steps are presented. After that, the used prognostics tool is introduced.

The proposed approach is applied to an electro-thermally actuated MEMS valve. For this purpose, an experimental platform is designed to validate the obtained nominal behavior model of the targeted MEMS, perform accelerated lifetime tests and derive its degradation model. In this work, the degradation of each MEMS was seen as a drift in its physical health indicator, which corresponds to its compliance. Once the degradation model is obtained, the SIR particle filter is used to perform online prognostics. This tool allowed to estimate the degradation model parameters, predict the future behavior of the MEMS and calculate its RUL. The obtained results clearly demonstrate the effectiveness of the proposed prognostics approach.

The estimated RUL values can be exploited to take appropriate decision on systems in which the MEMS are used. However, this aspect is not addressed in this contribution. Thus, as a future work, it is expected to implement this approach on a real application, including the decision part. The application consists in a centimeter contact-less distributed MEMS-based conveying surface. It is dedicated for distributed post-prognostics decision making and aims at optimizing the utilization of the conveying surface, maintaining a good performance as long as possible and avoiding loss or damage of transported micro-objects.

References

[1] K. Medjaher, H. Skima, N. Zerhouni, Condition assessment and fault prognostics of microelectromechanical systems, Microelectronics Reliability 54 (2014) 143–151.

[2] J. Li, M. Broas, J. Raami, T. T. Mattila, M. Paulasto-Kröckel, Reliability assessment of a MEMS microphone under mixed flowing gas environment

and shock impact loading, Microelectronics Reliability 54 (6) (2014) 1228–1234.

[3] J. A. Walraven, Failure analysis issues in microelectromechanical systems (MEMS), Microelectronics Reliability 45 (2005) 1750–1757.

[4] M. McMahon, J. Jones, A methodology for accelerated testing by mechanical actuation of MEMS devices, Microelectronics Reliability 52 (2012) 1382–1388.

[5] D. Tanner, MEMS reliability: Where are we now?, Microelectronics reliability 49 (2009) 937–940.

[6] H. Tilmans, J. De Coster, P. Helin, V. Cherman, A. Jourdain, P. De Moor, B. Vandevelde, N. Pham, J. Zekry, A. Witvrouw, et al., MEMS packaging and reliability: An undividable couple, Microelectronics Reliability 52 (9) (2012) 2228–2234.

[7] D. M. Tanner, N. F. Smith, L. W. Irwin, W. P. Eaton, K. Helgesen, J. Clement, W. Miller, J. Walraven, K. Peterson, P. Tangyunyong, et al., MEMS reliability: infrastructure, test structures, experiments, and failure modes, SANDIA report (2000) 155–157.

[8] D. M. Tanner, T. B. Parson, A. D. Corwin, J. A. Walraven, J. W. Wittwer, B. L. Boyce, S. Winzer, Science-based MEMS reliability methodology, Microelectronics Reliability 47 (9) (2007) 1806–1811.

[9] K. C. Kapur, M. Pecht, Reliability engineering, John Wiley & Sons, 2014.

[10] M. Pecht, Prognostics and health management of electronics, Wiley Online Library, 2008.

[11] J. Lee, F. Wu, W. Zhao, M. Ghaffari, L. Liao, D. Siegel, Prognostics and health management design for rotary machinery systemsreviews, methodology and applications, Mechanical Systems and Signal Processing 42 (1) (2014) 314–334.

[12] M. Matmat, F. Coccetti, A. Marty, R. Plana, C. Escriba, J.-Y. Fourniols, D. Esteve, Capacitive RF MEMS analytical predictive reliability and lifetime characterization, Microelectronics Reliability 49 (9) (2009) 1304–1308.

[13] M. Matmat, K. Koukos, F. Coccetti, T. Idda, A. Marty, C. Escriba, J.-Y. Fourniols, D. Estève, Life expectancy and characterization of capacitive RF MEMS switches, Microelectronics Reliability 50 (9) (2010) 1692–1696.

[14] A. Saxena, J. Celaya, E. Balaban, K. Goebel, B. Saha, S. Saha, M. Schwabacher, Metrics for evaluating performance of prognostic techniques, in: Prognostics and health management (PHM) 2008, IEEE International conference on, IEEE, 2008, pp. 1–17.

[15] M. S. Arulampalam, S. Maskell, N. Gordon, T. Clapp, A tutorial on particle filters for online nonlinear/non-gaussian bayesian tracking, Signal Processing, IEEE Transactions on 50 (2) (2002) 174–188.

[16] N. J. Gordon, D. J. Salmond, A. F. Smith, Novel approach to nonlinear/non-gaussian bayesian state estimation, in: IEE Proceedings F (Radar and Signal Processing), Vol. 140, IET, 1993, pp. 107–113.

[17] B. Saha, K. Goebel, S. Poll, J. Christophersen, Prognostics methods for battery health monitoring using a bayesian framework, Instrumentation and Measurement, IEEE Transactions on 58 (2) (2009) 291–296.

[18] D. An, J.-H. Choi, N. H. Kim, Prognostics 101: A tutorial for particle filter-based prognostics algorithm using matlab, Reliability Engineering & System Safety 115 (2013) 161–169.

[19] M. E. Orchard, G. J. Vachtsevanos, A particle-filtering approach for online fault diagnosis and failure prognosis, Transactions of the Institute of Measurement and Control (2009) 221–246.

[20] T. Li, M. Bolic, P. Djuric, Resampling methods for particle filtering: Classification, implementation, and strategies, Signal Processing Magazine, IEEE 32 (3) (2015) 70–86.

[21] L. Guo, Y. Peng, D. Liu, Y. Luo, Comparison of resampling algorithms for particle filter based remaining useful life estimation, in: Prognostics and Health Management (PHM), 2014 IEEE Conference on, IEEE, 2014, pp. 1–8.

[22] B. Saha, K. Goebel, Model adaptation for prognostics in a particle filtering framework, International Journal of Prognostics and Health Management Volume 2 (color) (2011) 61.

[23] M. Dkhil, M. Kharboutly, A. Bolopion, S. Regnier, M. Gauthier, Closed-loop control of a magnetic particle at the air–liquid interface, Automation Science and Engineering, IEEE Transactions on PP (99) (2015) 1–13.

[24] M. K. Pitt, R. dos Santos Silva, P. Giordani, R. Kohn, On some properties of markov chain monte carlo simulation methods based on the particle filter, Journal of Econometrics 171 (2) (2012) 134–151.

[25] K. Javed, R. Gouriveau, N. Zerhouni, D. Hissel, Improving accuracy of long-term prognostics of pemfc stack to estimate remaining useful life, in: Industrial Technology (ICIT), 2015 IEEE International Conference on, 2015, pp. 1047–1052.